

## DNA Polymerase $\kappa$ Is Specifically Required for Recovery from the Benzo[*a*]pyrene-Dihydrodiol Epoxide (BPDE)-induced S-phase Checkpoint\*

Received for publication, February 10, 2005, and in revised form, April 5, 2005  
Published, JBC Papers in Press, April 6, 2005, DOI 10.1074/jbc.M501562200

Xiaohui Bi<sup>‡</sup>, Damien M. Slater<sup>‡</sup>, Haruo Ohmori<sup>§</sup>, and Cyrus Vaziri<sup>‡1</sup>

From the <sup>‡</sup>Department of Genetics and Genomics, Boston University School of Medicine, Boston, Massachusetts 02118 and <sup>§</sup>Institute for Virus Research, Kyoto University, 53 Shogoin-Kawaracho, Sakyo-ku, Kyoto 606-8507, Japan

Previously we identified an intra-S-phase cell cycle checkpoint elicited by the DNA-damaging carcinogen benzo[*a*]pyrene-dihydrodiol epoxide (BPDE). Here we have investigated the roles of lesion bypass DNA polymerases pol $\kappa$  and pol $\eta$  in the BPDE-induced S-phase checkpoint. BPDE treatment induced the re-localization of an ectopically expressed green fluorescent protein-pol $\kappa$  fusion protein to nuclear foci containing sites of active DNA synthesis in human lung carcinoma H1299 cells. In contrast, a similarly expressed yellow fluorescent protein-pol $\eta$  fusion protein showed a constitutive nuclear focal distribution at replication forks (in the same cells) that was unchanged in response to BPDE. BPDE-induced formation of green fluorescent protein-pol $\kappa$  nuclear foci was temporally coincident with checkpoint-mediated S-phase arrest. Unlike “wild-type” cells, *Polk*<sup>−/−</sup> mouse embryonic fibroblasts (MEFs) failed to recover from BPDE-induced S-phase arrest, while exhibiting normal recovery from S-phase arrest induced by ionizing radiation and hydroxyurea. XPV fibroblasts lacking pol $\eta$  showed a normal S-phase checkpoint response to BPDE (but failed to recover from the UV light-induced S-phase checkpoint), in sharp contrast to *Polk*<sup>−/−</sup> MEFs. The persistent S-phase arrest in BPDE-treated *Polk*<sup>−/−</sup> cells was associated with increased levels of histone  $\gamma$ H2AX (a marker of DNA double-strand breaks (DSBs)) and activation of the DSB-responsive kinases ATM and Chk2. These data suggest that in the absence of pol $\kappa$ , replication forks stall at sites of damage and collapse and generate DSBs. Therefore, we conclude that the trans-lesion synthesis enzyme pol $\kappa$  is specifically required for normal recovery from the BPDE-induced S-phase checkpoint.

Polycyclic aromatic hydrocarbons such as benzo[*a*]pyrene (B[a]P)<sup>1</sup> are ubiquitous environmental pollutants that elicit

DNA damage, mutagenesis, and carcinogenesis (1). The mechanism of B[a]P-induced carcinogenesis has been studied extensively and is well understood (4). B[a]P and other polycyclic aromatic hydrocarbons undergo intracellular oxidation reactions that generate reactive metabolites such as B[a]P-dihydrodiol epoxide (BPDE). BPDE is the “ultimate carcinogen” that results from B[a]P metabolism and forms a covalent linkage mainly with the exocyclic amino group of deoxyguanosine to form a bulky hydrophobic adduct (5). Error-prone replication of adducted DNA templates during S-phase can generate mutations. Potentially, mutations that activate oncogenes or inactivate tumor-suppressor genes can contribute to multistep carcinogenesis (2, 3).

Chromosomal DNA is continuously exposed to genotoxic insults from both endogenous and exogenous sources. Therefore, cells have evolved various mechanisms to minimize the detrimental effects of DNA damage. Cell cycle checkpoints are signal transduction mechanisms that respond to DNA damage by exerting negative controls over cell cycle progression (4). The cell cycle delays triggered by checkpoints enable integration of DNA repair with cell cycle progression following acquisition of DNA damage. Cell cycle checkpoint pathways can arrest cells at the G<sub>1</sub>/S transition, within S-phase (termed the “S-phase checkpoint” or “intra-S-phase checkpoint”), and at G<sub>2</sub>/M. It is widely hypothesized that cell cycle checkpoints are important tumor-suppressive mechanisms that contribute to the maintenance of genomic stability. Consistent with this hypothesis, individuals with congenital defects in checkpoint genes (*e.g.* *p53*, *CHK2*, and *ATM*) show increased propensity to tumorigenesis.

Many components of cell cycle checkpoint signaling cascades have been identified. It is now clear that partially separable checkpoint pathways respond to different forms of DNA damage. For example, DNA double strand breaks (DSB) activate the proximal ATM kinase that signals through the downstream kinase Chk2 and other effectors (5). In contrast, bulky DNA lesions (such as UV light-induced pyrimidine dimers or BPDE adducts) or replication stress (resulting from depletion of nucleotide pools) elicits a checkpoint pathway mediated by the ATM-related kinase ATR and its downstream effector kinase Chk1 (6). The mechanism by which DNA damage activates ATM is poorly understood but might involve direct interactions between ATM and damaged chromatin (7). In contrast, activation of ATR involves its recruitment to RPA-coated single-stranded DNA via the ATR-interacting protein ATRIP (also known as Rad26) (8, 9).

\* This work was supported in part by a grant-in-aid from the Ministry of Education, Culture, Sports, Science and Technology of Japan (to H. O.) and by NIEHS Grants ES09558 and ES12917 from the National Institutes of Health (to C. V.). The costs of publication of this article were defrayed in part by the payment of page charges. This article must therefore be hereby marked “advertisement” in accordance with 18 U.S.C. Section 1734 solely to indicate this fact.

<sup>1</sup> To whom correspondence should be addressed: Dept. of Genetics and Genomics, Boston University School of Medicine, 80 E. Concord St., Boston, MA 02118. Tel.: 617-638-4175; Fax: 617-414-1646; E-mail: cvaziri@bu.edu.

<sup>2</sup> The abbreviations used are: B[a]P, benzo[*a*]pyrene; BPDE, benzo[*a*]pyrene-dihydrodiol epoxide; GFP, green fluorescent protein; YFP, yellow fluorescent protein; MEFs, mouse embryonic fibroblasts; pol, polymerase; DSB, double-strand break; FACS, fluorescence-activated cell sorter; PBS, phosphate-buffered saline; BSA, bovine serum albumin; DAPI, 4,6-diamidino-2-phenylindole; BrdUrd, bromodeoxyuridine; RFC, replication factor C; PCNA, proliferating cell nuclear antigen; HDFs, human dermal fibroblasts; TLS, trans-lesion synthesis; XPV, xeroderma pigmentosum-variant; CMV, cytomegalovirus; WT, wild type.

Additional key mammalian DNA damage-response factors required for Chk1 activation are Rad17 and Rad9-Rad1-Hus1 (which form a heterotrimeric complex termed "9-1-1") (10, 11). Rad17 resembles the replication factor C (RFC) I subunit and similarly forms a complex with RFC subunits II–V. The RFC I–V complex is responsible for loading the PCNA sliding clamp onto DNA during the elongation step of DNA synthesis. Each of the 9-1-1 subunits bears similarity with PCNA, and analogously, the 9-1-1 complex is thought to form a "clamp" that associates with DNA (12). The association of 9-1-1 with damaged DNA is regulated by the concerted actions of Rad17 and RFC subunits II–V (12). Although 9-1-1 and ATR/ATRIP are recruited to chromatin via separate mechanisms (13), both events are required for Chk1 activation and checkpoint signaling. When activated, Chk1 contributes to cell cycle arrest in S-phase and G<sub>2</sub>/M. The Chk1-mediated G<sub>2</sub> arrest is mediated via negative regulation of the Cdc25C protein phosphatase (14). The mechanism of Chk1-mediated S-phase arrest is less clear but might involve degradation of the Cdc25A protein phosphatase (15, 16) and inhibition of Cdc7-Dbf4 kinase complex (17).

S-phase checkpoints are considered to be important for coordinating DNA synthesis with DNA repair after acquisition of DNA damage during S-phase (18). Replicative DNA polymerases do not copy damaged DNA templates efficiently or accurately. Therefore, cells use the following two mechanisms to replicate loci containing DNA damage: 1) recombinational repair using the undamaged sister chromatid DNA as a template for the sequence opposite the lesion; 2) specialized DNA polymerases can be used to replicate past lesions in a process termed trans-lesion synthesis (TLS). Recombinational repair is an error-free mechanism (19, 20). In contrast, because of the low fidelity of TLS DNA polymerases, replicative bypass of lesions is an inherently error-prone process (21–23). Indeed, TLS is considered to be the reason for mutagenesis and carcinogenesis in response to DNA lesions.

Major TLS DNA polymerases in mammalian cells are pol $\kappa$ , pol $\eta$ , pol $\iota$ , and Rev1 (the "Y" family polymerases) and pol $\zeta$  (a "B" family polymerase comprising the catalytic Rev3 subunit and the noncatalytic Rev7 protein). pol $\eta$  was the first mammalian TLS polymerase identified (24). pol $\eta$  is encoded by the *XPV* gene, which is defective in xeroderma pigmentosum-variant patients. The role of mammalian pol $\eta$  (and of its *Saccharomyces cerevisiae* homologue Rad30) in TLS has been studied extensively. pol $\eta$  is unique among eukaryotic DNA polymerases in its ability to replicate through a *cis-syn* thymine-thymine dimer (the species generated by UV radiation). Studies *in vitro* and *in vivo*, in yeast and mammalian systems, indicate that pol $\eta$  promotes error-free DNA trans-lesion synthesis in a manner that is stimulated by PCNA and regulated by the Rad6/Rad18 epistasis pathways (25, 26).

Genes encoding the Y family enzyme DNA polymerase  $\kappa$  (pol $\kappa$ ) were originally identified as human and murine homologues of *Escherichia coli* DinB (now termed polIV) (27). Unlike human pol $\eta$ , human pol $\kappa$  and *E. coli* polIV are unable to bypass UV light-induced DNA lesions. However, both pol $\kappa$  and polIV are able to bypass benzo[a]pyrene-adducted guanine, efficiently inserting the correct "C" opposite the bulky lesion (28). Consistent with a role for pol $\kappa$  in cellular responses to B[a]P-induced genotoxicity, pol $\kappa$ -deficient mutant mouse embryonic stem cells are highly sensitive to B[a]P, showing an elevated mutation frequency and its spectrum different from that in the parental cell (29). Bergoglio *et al.* (30) reported that hydroxyurea and UV light irradiation can elicit recruitment of pol $\kappa$  to nuclear foci, suggesting a possible role for pol $\kappa$  in responses to genotoxins and replication stress. Like pol $\eta$ , pol $\kappa$  interacts phys-

ically with PCNA, and its DNA synthesis activity is stimulated by PCNA and RFC *in vitro* (31).

Therefore, there is good evidence that Y family polymerases play key roles in the regulation of DNA synthesis after acquisition of DNA damage. However, thus far, S-phase checkpoint pathways and TLS processes have been studied completely separately, and the relationships between the two cellular processes remain totally unknown. In this study we have tested roles for TLS polymerases in the S-phase checkpoint elicited by BPDE. Previous work from our laboratory has demonstrated that the ATR/9-1-1/Chk1 pathway mediates S-phase arrest in response to BPDE adducts (32, 33). Because of results from other laboratories demonstrating roles for pol $\kappa$  in replicative bypass of BPDE adducts *in vitro* and cell survival after B[a]P challenge, we tested a potential role for pol $\kappa$  in the BPDE-induced intra-S-phase checkpoint. The results presented here demonstrate that pol $\kappa$  is recruited to sites of ongoing DNA synthesis after acquisition of BPDE damage. Furthermore, we show that pol $\kappa$  is required for a normal S-phase checkpoint in response to BPDE adducts (and UV light-induced lesions) but not S-phase checkpoints because of DSBs or replication stress. In contrast, pol $\eta$  is dispensable for the BPDE-induced checkpoint, yet is required for a normal checkpoint response to UV lesions.

#### MATERIALS AND METHODS

**Adenovirus Construction**—cDNAs encoding GFP-pol $\kappa$  and YFP-pol $\eta$  were subcloned into pAC-CMV to generate pAC-GFP-pol $\kappa$  and pAC-YFP-pol $\eta$ , respectively. The resulting shuttle vectors were co-transfected into 293T cells with the pJM17 plasmid to generate recombinant adenovirus as described previously (32).

**Cell Culture**—Human lung carcinoma H1299 cells, Pol $\kappa^{+/+}$ , and Pol $\kappa^{-/-}$  mouse embryonic fibroblasts (MEFs) and xeroderma pigmentosum-variant CRL1162 fibroblasts or CRL1162 + XPV (XPV cells reconstituted with pol $\eta$ ) were cultured in Dulbecco's modified Eagle's medium supplemented with 10% fetal bovine serum and streptomycin sulfate (100  $\mu$ g/ml) and penicillin (100 units/ml).

**Genotoxin Treatments**—BPDE (NCI carcinogen repository) was dissolved in anhydrous Me<sub>2</sub>SO and added directly to the growth medium as a 1000 $\times$  stock to give final concentrations of 100 or 600 nM. For hydroxyurea treatment, hydroxyurea was dissolved in water and added directly to the growth medium as a 1000 $\times$  stock to give a final concentration of 1  $\mu$ M. For UVC treatment, the growth medium was removed from the cells and replaced with PBS. The plates were transferred to a UV cross-linker (Stratagene) and then irradiated. The UVC dose delivered to the cells was confirmed with a UV radiometer (UVP, Inc.). The cells were then re-fed with complete growth medium and returned to the incubator. For IR treatment, cells were placed in PBS, irradiated with a cesium source, then re-fed with complete growth medium, and returned to the incubator. In some experiments, cells were incubated in medium containing 5 mM caffeine (Sigma) for 1 h before genotoxin treatment.

**Clonogenic Survival Assays**—For colony survival assays, cells were grown to 80% confluence, treated with genotoxins (as described above), and then split into replicate 10-cm plates at a density of 1000 cells/plate. Plates were re-fed every 3 days. After 10 days, colonies on the plates were fixed in methanol, stained with crystal violet, and counted.

**DNA Synthesis Assays**—[<sup>3</sup>H]Thymidine incorporation assays were performed as described previously (32, 33). In brief, cells were split into 12-well plates and grown to 60% confluence. After genotoxin treatments, replicate wells were given [<sup>3</sup>H]thymidine (1  $\mu$ Ci/ml, PerkinElmer Life Sciences) for 30 min. At the end of the labeling period, the [<sup>3</sup>H]thymidine-containing medium was aspirated, and the monolayers were fixed by addition of 5% trichloroacetic acid. The fixed cells were washed three times with 5% trichloroacetic acid to remove unincorporated [<sup>3</sup>H]thymidine. The trichloroacetic acid-fixed cells were solubilized in 0.3 N NaOH. A 300- $\mu$ l aliquot of the NaOH-solubilized material was transferred to a scintillation vial and neutralized by addition of 100  $\mu$ l of glacial acetic acid. After addition of 5 ml of Ecoscint scintillation fluid, [<sup>3</sup>H]thymidine was measured by scintillation counting.

**FACS Analysis**—Cells were split into 60-mm plates and grown to 60% confluence. Cells were pulsed with BrdUrd for 1 h to label the S-phase population. The resulting cultures were washed three times with 5 ml of complete medium to remove unincorporated BrdUrd.



Genotoxin treatments were as described above. Labeling and FACS analyses were performed as described previously (34). At various times after genotoxin treatment, cells were trypsinized, recovered by centrifugation ( $10,000 \times g$ , 30 s), and fixed in 35% EtOH in PBS for 1 h overnight. Fixed nuclei were recovered by centrifugation and incubated in 2 N HCl for 20 min to denature the DNA. Acid-treated cells were neutralized by washing in 0.1 M borax, pH 8.5, and then rinsed in PBS. The resulting pellets were resuspended in 50  $\mu$ l of antibody labeling solution comprising 30  $\mu$ l of PBS with 0.5% Tween 20 and 0.5% BSA plus 20  $\mu$ l of fluorescein isothiocyanate-conjugated BrdUrd antibody (Pharmingen). The cells were incubated for 30 min in the dark with frequent mixing. Labeled cells were resuspended and washed in 1 ml of PBS to remove free antibody. Washed nuclei were resuspended in 1 ml of PBS containing 8  $\mu$ g of RNase A and 50  $\mu$ g of propidium iodide. The nuclear suspensions were incubated in the dark at room temperature for 30 min prior to FACS analysis (on a BD Bioscience instrument with Cellquest software).

**Fluorescence Microscopy**—Cells were split into 4-well chamber slides, grown to 50% confluence, and then infected with adenovirus carrying GFP-*polk* or YFP-*pol* $\eta$ . 20 h after infection, cells were treated with genotoxins for various times. To visualize GFP-*polk* or YFP-*pol* $\eta$  fluorescence, the cells were fixed with 4% paraformaldehyde for 10 min and then permeabilized with 0.2% Triton X-100 for 5 min. After washing the slides with PBS, cells were DAPI-stained and mounted with Vectashield solution (Vector Laboratories). For some experiments, sites of ongoing DNA synthesis were labeled by incubation in 35  $\mu$ M BrdUrd-containing medium for 20 min, immediately prior to genotoxin treatment. To detect incorporated BrdUrd, the fixed cells were treated with 2 N HCl (to denature the DNA) after fixation. After neutralization and washing in PBS, cells were incubated overnight at 4 °C with a mouse monoclonal anti-BrdUrd antibody (Serotec) diluted 1:10 in 1% BSA/PBST. The slides were washed three times with 1% BSA/PBST and then incubated for 1 h with Cy3-conjugated donkey anti-mouse antibodies (Jackson ImmunoResearch) diluted 1:300 in 1% BSA/PBST. After washing (three times with 1% BSA/PBST), the slides were DAPI-stained and mounted with Vectashield solution (Vector Laboratories). Slides were imaged and analyzed using a Delta Vision Image Restoration Microscopy System (dv1301421, Applied Precision). In some experiments cell populations were scored for constitutive and genotoxin-induced foci using a Nikon Eclipse E800 fluorescent microscope. In these studies, 500 cells were counted for each experimental condition.

**Immunoblotting**—Total cell lysates were prepared as described previously (32) in lysis buffer containing 50 mM Hepes, pH 7.4, 0.1% Triton X-100, 150 mM NaCl, 1 mM EDTA, 50 mM NaF, 80 mM  $\beta$ -glycerophosphate, and 1 $\times$  protease inhibitor mixture (Roche Applied Science). In some experiments, whole nuclei were prepared using CSK buffer as described by Hanaoka and co-workers (35). Total cell extracts or nuclear protein samples were separated by SDS-PAGE, transferred to nitrocellulose, and analyzed using the following antibodies: rabbit anti-Chk1 (FL-476, Santa Cruz Biotechnology), rabbit anti-Chk2 (H-300, Santa Cruz Biotechnology), mouse monoclonal PCNA (sc-56, Santa Cruz Biotechnology), rabbit anti-phospho-Chk1 Ser-345 (catalog number 2341, Cell Signaling), rabbit anti-phospho-Chk2 Thr-68 (catalog number 2661, Cell Signaling), mouse monoclonal anti-phospho-ATM Ser-1981 (catalog number 4526, Cell Signaling), and mouse monoclonal anti-phospho-H2AX (catalog number 05-636, Upstate Biotechnology Inc.).

**Reproducibility**—All data shown are representative of experiments that were repeated at least three times in replicate.

## RESULTS

**BPDE Induces Formation of GFP-*polk* Nuclear Foci at Sites of Ongoing DNA Synthesis**—Other workers have shown (30, 36) that a fusion protein of *polk* with GFP is recruited to discrete nuclear foci (presumably representing sites of DNA damage) in response to genotoxins. However, the effect of BPDE on the subcellular distribution of *polk* has not been studied in detail. Therefore, we investigated GFP-*polk* localization during the BPDE-induced S-phase checkpoint response.

For expression of GFP-*polk* in cultured cells, we generated a recombinant adenovirus vector (designated AdGFP-*polk*). We chose human lung carcinoma H1299 cells for our studies of GFP-*polk* distribution because we have characterized S-phase regulation extensively in this cell line (32, 34). More importantly, we have shown that H1299 cells contain an intact

BPDE-induced S-phase checkpoint pathway (32).

Exponentially growing H1299 cells were infected with AdGFP-*polk* at a multiplicity of infection of 5 per cell, which results in 100% transduction efficiency under our standard experimental conditions. 18 h after infection of H1299 cells with AdGFP-*polk*, the GFP-*polk* fusion protein displayed a diffuse nuclear distribution. A representative GFP-*polk*-expressing H1299 cell is shown in the *upper left panel* of Fig. 1*a*. Next we tested the effect of BPDE treatment on *polk* localization. AdGFP-*polk*-expressing cells were treated with 100 nM BPDE for 2 or 20 h. At 2 h after treatment with 100 nM BPDE, H1299 cells undergo a transient inhibition of DNA synthesis (Fig. 1*b*). The BPDE-induced delay in S-phase results from inhibition of initiation of DNA synthesis at late-firing origins (37, 38) and is termed the intra-S-phase checkpoint. 6–8 h after treatment with 100 nM BPDE, cells recover from the checkpoint-mediated inhibition of DNA synthesis (Fig. 1*b*).

Concomitant with activation of the BPDE-induced checkpoint, we observed an increase in the formation of nuclear GFP-*polk* foci. A representative cell containing GFP-*polk* foci is shown in Fig. 1*a* (*middle left panel*). Approximately 50% of the cells contained GFP-*polk* foci 2 h after treatment with 100 nM BPDE (Fig. 1*c*). The nuclear GFP-*polk* foci resulting from 100 nM BPDE were induced transiently. 20 h after 100 nM BPDE treatment, a time point after the cells recover from the BPDE-induced S-phase checkpoint (Fig. 1*b*), few GFP-*polk* foci were evident. Therefore, there is a good temporal correlation between checkpoint-mediated inhibition of DNA synthesis and recruitment of GFP-*polk* to sites of damage.

Doses of 600 nM BPDE or higher induce an irreversible block to DNA synthesis (Fig. 1*b*). Inhibition of DNA synthesis by high doses of BPDE (~600 nM) resulted from inhibition of origin firing (initiation) and chain elongation (37, 38). In contrast with the checkpoint-mediated inhibition of initiation, the block to elongation was not considered a checkpoint response but instead resulted from direct physical blocks to DNA replication at sites of damage. Treatment of GFP-*polk*-expressing H1299 cells with 600 nM BPDE resulted in more numerous and intense nuclear foci than were induced by 100 nM BPDE. Moreover, foci induced by 600 nM BPDE were present for at least 20 h, concomitant with BPDE-induced replication blocks (Fig. 1, *a*, *right panels*, and *c*).

As indicated in Fig. 1*c*, GFP-*polk* foci were detected in ~50% of the genotoxin-treated cells 2 h after acquisition of DNA damage. In exponentially growing cultures of H1299 cells, ~50% of the population was actively synthesizing DNA, as shown by BrdUrd labeling and FACS analysis (Fig. 2*a*). Therefore, it appeared likely that the cells containing BPDE-induced *polk* foci represented those actively synthesizing DNA.

To identify S-phase sub-populations of GFP-*polk*-expressing cells, the cultures were pulse-labeled in the presence of BrdUrd for 1 h immediately prior to treatment with genotoxins. After genotoxin treatment, BrdUrd incorporated into S-phase nuclei was visualized using Cy3-coupled secondary antibodies (Fig. 2*b*). In these experiments, BPDE-induced GFP-*polk* nuclear foci were only ever detected in BrdUrd-positive cells (Fig. 2*b*), thereby demonstrating that nuclear *polk* focus formation occurs in S-phase. Moreover, GFP-*polk* foci localized adjacent to sites that were pre-labeled with BrdUrd, (*i.e.* replication foci), suggesting that nuclear *polk* foci represent sites where active replication forks encounter BPDE adducts.

**Effect of BPDE on Nuclear Focus Formation by *pol* $\eta$ —*pol* $\eta$** , the product of the XPV gene, is important for TLS of UV light-induced adducts (24). Kannouche and co-workers (39, 40) have shown that GFP or YFP fusions of *pol* $\eta$  are recruited to nuclear foci in response to UV light-induced lesions, as well as other

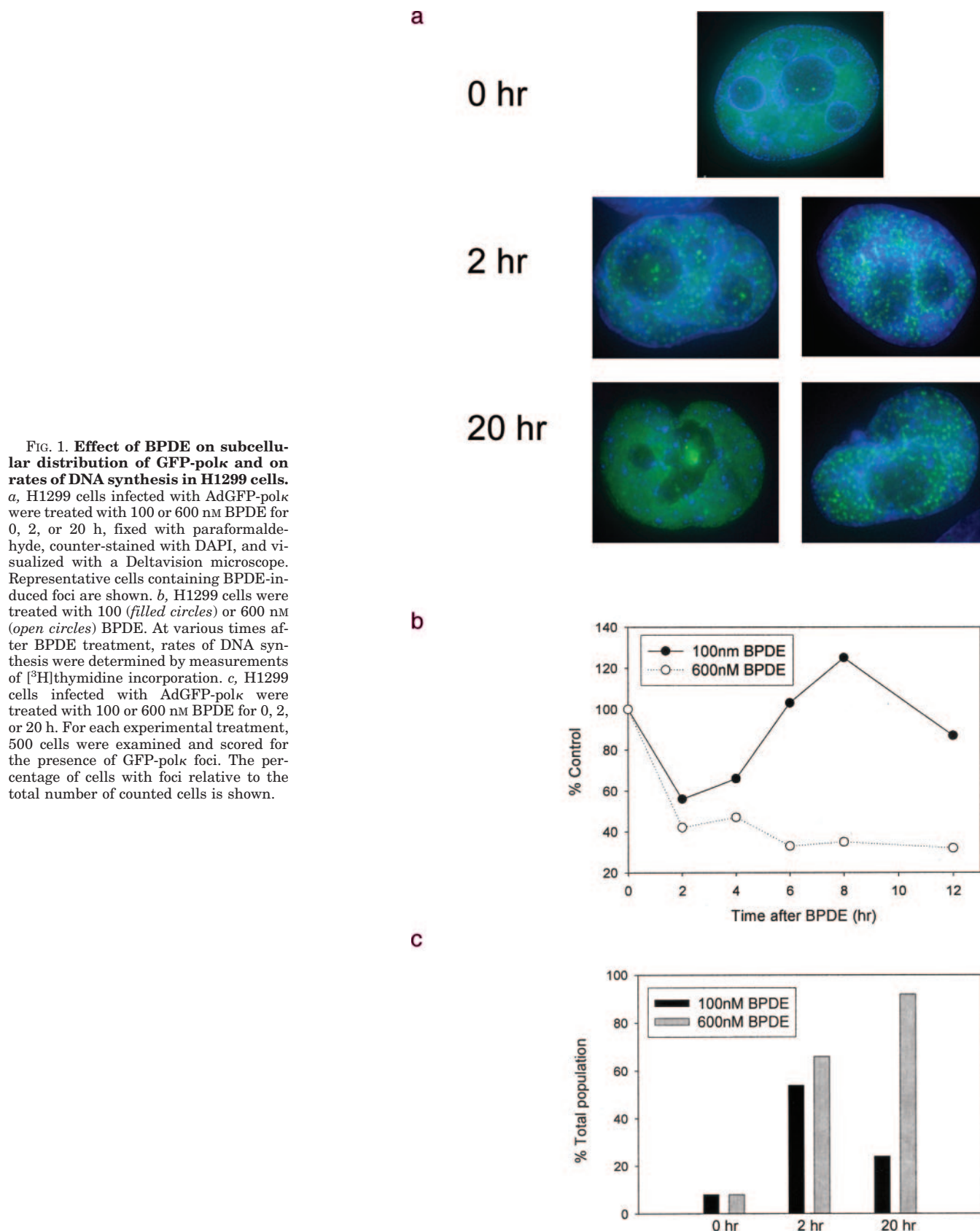


**FIG. 1. Effect of BPDE on subcellular distribution of GFP-pol $\kappa$  and on rates of DNA synthesis in H1299 cells.** *a*, H1299 cells infected with AdGFP-pol $\kappa$  were treated with 100 or 600 nM BPDE for 0, 2, or 20 h, fixed with paraformaldehyde, counter-stained with DAPI, and visualized with a Deltavision microscope. Representative cells containing BPDE-induced foci are shown. *b*, H1299 cells were treated with 100 (filled circles) or 600 nM (open circles) BPDE. At various times after BPDE treatment, rates of DNA synthesis were determined by measurements of [ $^3$ H]thymidine incorporation. *c*, H1299 cells infected with AdGFP-pol $\kappa$  were treated with 100 or 600 nM BPDE for 0, 2, or 20 h. For each experimental treatment, 500 cells were examined and scored for the presence of GFP-pol $\kappa$  foci. The percentage of cells with foci relative to the total number of counted cells is shown.

forms of DNA damage. However, the effect of BPDE on the subcellular distribution of pol $\eta$  has not been reported. UV light-induced TT dimers and BPDE adducts are both repaired via the nucleotide excision repair pathway, and both activate an ATR/Chk1-mediated S-phase checkpoint. Therefore, we asked if

BPDE adducts induced nuclear pol $\eta$  foci. We generated a recombinant adenovirus vector for expression of YFP-pol $\eta$  (designated AdYFP-pol $\eta$ ). H1299 cells were infected with AdYFP-pol $\eta$ , and pol $\eta$  distribution was determined by microscopy. Most interestingly, and in contrast with GFP-pol $\kappa$ , the YFP-pol $\eta$  fusion protein

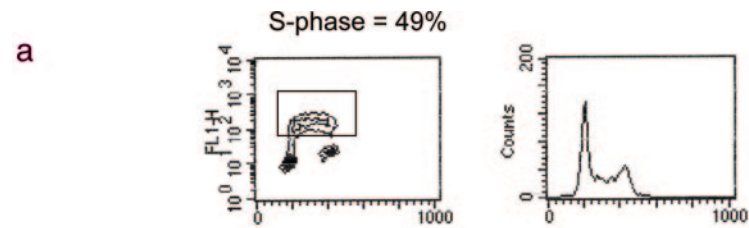
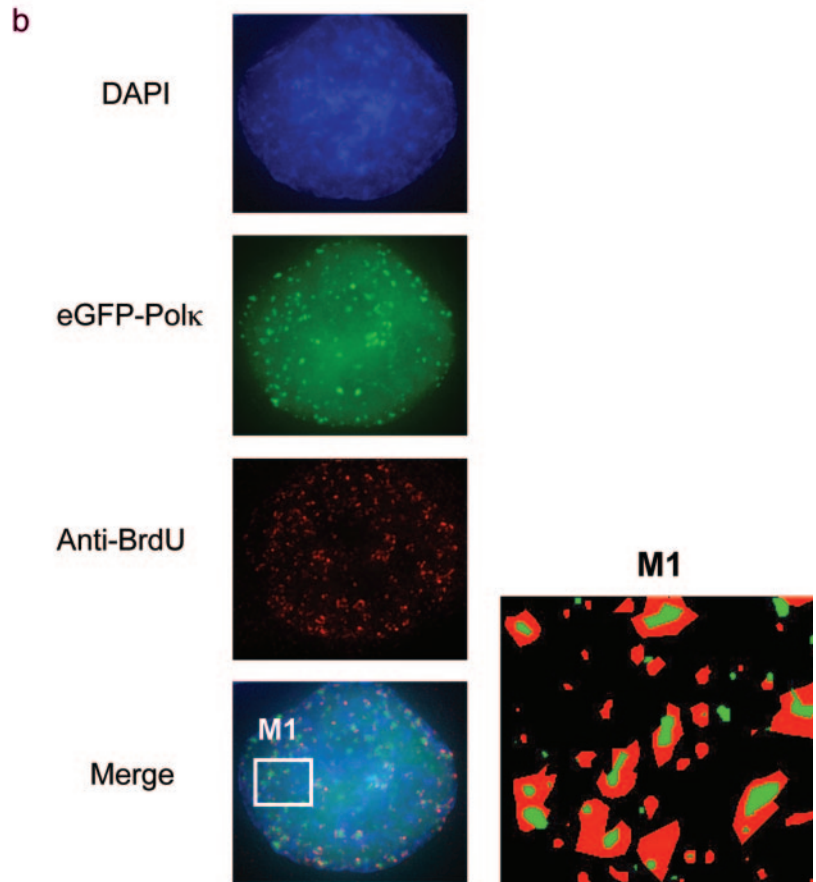


**FIG. 2. Formation of GFP-*polk* foci in S-phase cells after BPDE treatment.** *a*, exponentially growing H1299 cells were pulsed with BrdUrd for 1 h. After trypsinization, the cells were fixed, permeabilized, stained with anti-BrdUrd antibodies and PI, and then analyzed by flow cytometry. *b*, H1299 cells infected with AdGFP-*polk* were labeled for 1 h with BrdUrd and then treated with 100 nM BPDE for 1 h. After fixing, the cells were stained with Cy3-conjugated anti-BrdUrd antibodies and visualized with a Deltavision microscope. A representative cell containing BrdUrd-labeled loci (red) and BPDE-induced GFP-*polk* foci (green) is shown (left-hand panels). The lower right-hand panel shows the results of a three-dimensional modeling analysis of subnuclear region M1. The Deltavision 3D object builder software was used to create a three-dimensional model from the two-dimensional polygons in each Z section of region M1. The schematic depicts the degree to which green (GFP-*polk*) and red (BrdUrd) signals co-localize in three dimensions.



localized to nuclear foci in the absence of genotoxin treatment. BrdUrd labeling experiments showed that YFP-*polη* foci were coincident with sites of DNA synthesis (data not shown). This finding is consistent with reports from other laboratories that *polη* is constitutively localized to the replication fork (39).

Treatment with BPDE, or other genotoxins (including UV light, hydroxyurea, IR), did not elicit increased YFP-*polη* focus formation in H1299 cells (Fig. 3*a*). This result contrasts with previous reports that GFP-*polη* forms nuclear foci in response to genotoxins in other cell types (39). To investigate this apparent discrepancy, we determined the effects of DNA-damaging agents on the subcellular localization of YFP-*polη* and GFP-*polκ* in additional cell types. H1299 cells are defective for p53-mediated G<sub>1</sub> and G<sub>2</sub> checkpoints. Therefore, we hypothesized that the constitutive YFP-*polη* foci in H1299 cells might result from high levels of spontaneous DNA damage caused by unchecked or un-repaired replication errors. H1299 cells show high basal levels of histone γH2AX as determined by immunofluorescence microscopy and Western blotting (data not shown), suggesting the presence of high levels of constitutive DNA damage under our experimental conditions.

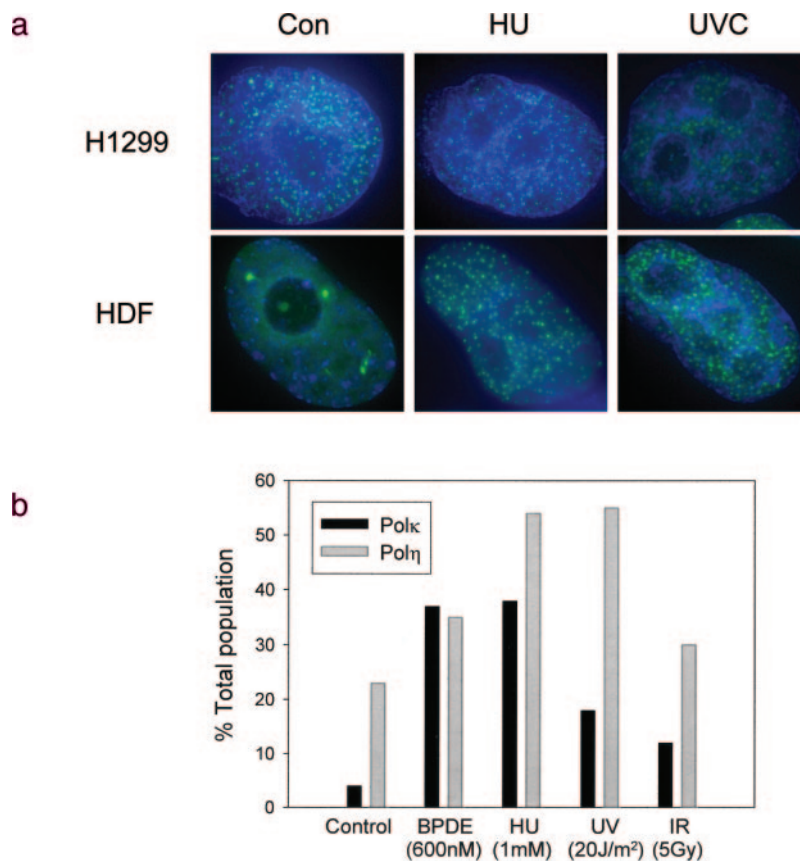
To ask if the presence of constitutive *polη* foci correlated with

a malignant phenotype, we investigated the subcellular distribution of *polη* (and also of *polκ*) in nontransformed primary human dermal fibroblasts in the absence or presence of different DNA lesions. Early passage primary human dermal fibroblasts (HDFs) were infected with adenovirus encoding YFP-*polη*. In contrast with H1299 cells, in which *polη* localized to nuclear foci in 100% of the population, *polη* localized to nuclear foci only in ~20% of the HDF cells in the absence of genotoxic insult. A representative cell showing diffuse nuclear distribution of *polη* in HDFs is shown in Fig. 3*a* (bottom left panel). In other experiments we have observed constitutive *polη* foci in several cancer cell lines but rarely in untransformed/primary cell lines (data not shown).

Because HDFs show low basal levels of *polη* foci, we determined the effects of BPDE and other genotoxins on the subcellular localization of YFP-*polη* and GFP-*polκ* in these cells. As shown in Fig. 3*b*, only 5% of GFP-*polκ*-expressing cells and 20% of YFP-*polη*-expressing cells contained nuclear foci in the absence of genotoxin treatment. However, 6 h after treatment with 600 nM BPDE, GFP-*polκ* and YFP-*polη* nuclear foci were present in 35 and 45% of the population, respectively. A 6-h treatment with hydroxyurea, an agent that depletes nucleotide



**FIG. 3. Subcellular distribution of YFP-*pol* $\eta$  in H1299 carcinoma cells.** *a*, H1299 or HDF cells infected with AdYFP-*pol* $\eta$  were treated with 1 mM hydroxyurea (HU) or 10 J/cm<sup>2</sup> UVC for 8 h, fixed with paraformaldehyde, counter-stained with DAPI, and visualized with a Deltavision microscope. *b*, HDFs were infected with AdGFP-*pol* $\kappa$  or AdYFP-*pol* $\eta$  and then treated with various genotoxins for 6 h as described in the text. Cells containing nuclear foci were scored as described under "Materials and Methods." *Con*, control; *Gy*, gray.



pools and causes stalled replication forks, also induced similar numbers of *pol* $\kappa$  and *pol* $\eta$  foci (38 and 55% of the population respectively). In contrast, 20 J/m<sup>2</sup> UVC elicited *pol* $\eta$  foci in 56% of the population, but under the same experimental conditions *pol* $\kappa$  foci were present in less than 20% of the population. Similar to UV irradiation, IR treatment induced greater numbers of *pol* $\eta$  foci (35%) than *pol* $\kappa$  foci (11%) in HDFs.

Taken together, our data show that *pol* $\eta$  (but not *pol* $\kappa$ ) constitutively localizes to nuclear foci in H1299 cells, possibly because of high spontaneous levels of DNA damage in this cell line. In primary untransformed HDFs, *pol* $\eta$  and *pol* $\kappa$  do not localize to nuclear foci in the absence of DNA damage, yet both polymerases form foci after treatment with genotoxins. However, quantitative differences are evident with respect to the relative numbers of *pol* $\kappa$  and *pol* $\eta$  foci induced by specific genotoxins in HDFs. Most notably, UV light and IR induce large numbers of *pol* $\eta$  foci, yet have modest effects on focus formation by *pol* $\kappa$  foci. These results suggest that *pol* $\kappa$  and *pol* $\eta$  play distinct roles in DNA synthesis during a normal S-phase and after acquisition of DNA lesions.

**Effect of Caffeine on Formation of *pol* $\kappa$  Foci**—Many DNA damage-induced responses are sensitive to inhibition by caffeine (41, 42). For example, we have demonstrated previously that the BPDE-induced S-phase checkpoint is abrogated by caffeine treatment (32). Therefore, it was of interest to us to determine the effect of caffeine on BPDE-induced *pol* $\kappa$  nuclear focus formation.

H1299 cells were infected with AdGFP-*pol* $\kappa$  and then treated for 1 h with 5 mM caffeine (or left untreated for controls). Replicate cultures of control and caffeine-treated cells were then given 100 nM BPDE (or left untreated) for 2 h. Then the GFP-*pol* $\kappa$  distribution in control, BPDE-treated, and BPDE + caffeine-treated cells was determined by microscopy. As expected, BPDE treatment induced GFP-*pol* $\kappa$  foci in cells that did not receive caffeine. Most interestingly, however, the numbers

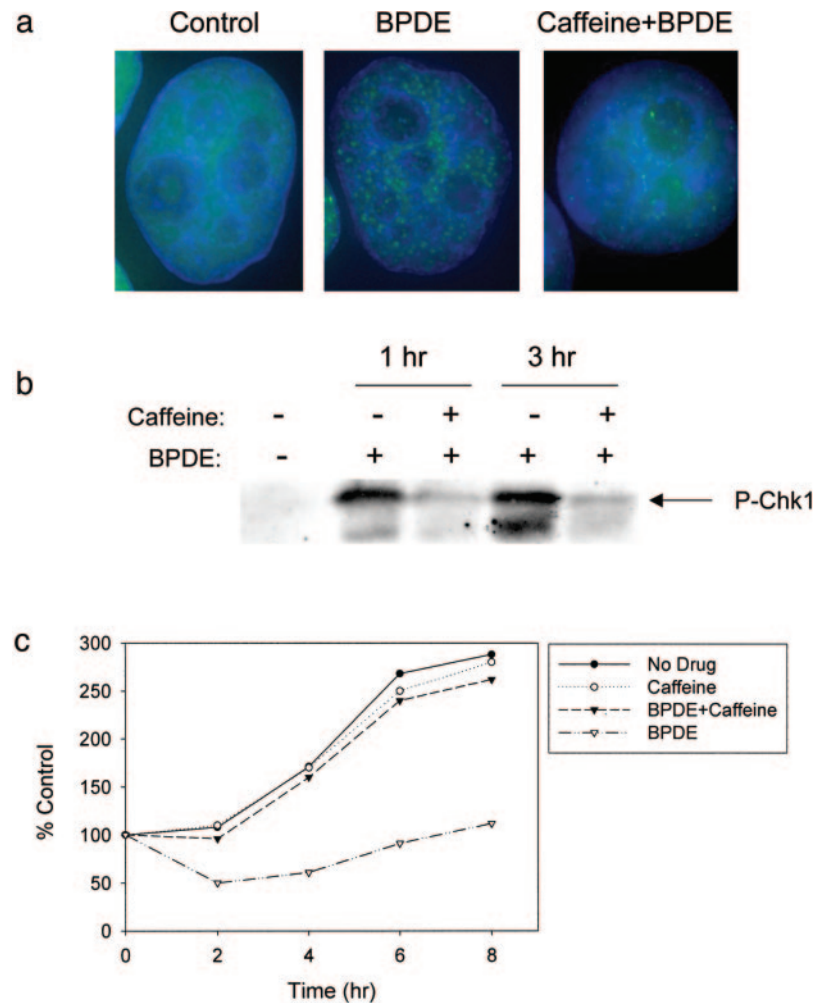
of BPDE-induced *pol* $\kappa$  foci formation were greatly reduced in caffeine-treated populations. The percentage of cells containing GFP-*pol* $\kappa$  foci was similar between BPDE- and BPDE + caffeine-treated cultures. Typically, however, caffeine + BPDE-treated cells contained 80% fewer foci compared with cells that received BPDE alone (e.g. Fig. 4a). Moreover, the few BPDE-induced GFP-*pol* $\kappa$  foci that were evident in caffeine-treated cells were less intense and more diffuse compared with foci in cultures that did not receive caffeine (Fig. 4a). In parallel experiments, caffeine treatment abrogated BPDE-induced Chk1 phosphorylation (Fig. 4b) and DNA damage-induced inhibition of thymidine incorporation (Fig. 4c), thereby demonstrating abrogation of the S-phase checkpoint pathway under our experimental conditions. Therefore, *pol* $\kappa$  regulation is perturbed by caffeine treatment. In similar experiments using AdYFP-*pol* $\eta$ -infected cells, basal and DNA damage-induced *pol* $\eta$  foci were unaffected by caffeine treatment. Our data suggested that the caffeine-sensitive kinases ATM and ATR might specifically mediate the BPDE-induced recruitment of GFP-*pol* $\kappa$  to nuclear foci. However, in unpublished experiments,<sup>2</sup> we have found that GFP-*pol* $\kappa$  forms nuclear foci in BPDE-treated AT cells (which lack functional ATM protein) and ATR-flox cells (in which the *Atr* gene is deleted). Therefore, a caffeine-sensitive process other than ATM/ATR-mediated signaling is involved in *pol* $\kappa$  regulation.

**Effect of *pol* $\kappa$  and *pol* $\eta$  Deficiency on the Intra-S-phase Checkpoint**—The effect of genotoxins on the subcellular localization of GFP-*pol* $\kappa$  in S-phase cells suggested a potential role for *pol* $\kappa$  in regulating cell cycle progression after acquisition of DNA damage. Therefore, we tested a possible role for *pol* $\kappa$  in the intra-S-phase checkpoint.

To test the role of *pol* $\kappa$  in the intra-S-phase checkpoint, we

<sup>2</sup> X. Bi, D. M. Slater, H. Ohmori, and C. Vaziri, unpublished data.

**FIG. 4. Abrogation of BPDE-induced GFP-*polk* foci, Chk1 phosphorylation, and S-phase arrest by caffeine.** *a*, H1299 cells infected with AdGFP-*polk* were treated with 2 mM caffeine or left untreated for controls. Control and caffeine-treated cultures were given 100 nM BPDE for 2 h before being fixed with paraformaldehyde, counterstained with DAPI, and visualized with a Deltavision microscope. Representative cells containing BPDE-induced foci are shown. *b*, exponentially growing H1299 cells were treated with 2 mM caffeine or left untreated for controls. Control and caffeine-treated cultures were given 100 nM BPDE for 1 or 3 h. Protein extracts from the resulting cells were separated by electrophoresis, blotted, and probed with anti-phospho-Ser-345 Chk1 antisera. *c*, exponentially growing H1299 cells were treated with 2 mM caffeine or left untreated for controls. At various times after BPDE treatment, rates of DNA synthesis were determined by measurements of [ $^3$ H]thymidine incorporation.



measured rates of DNA synthesis in *Polk*<sup>-/-</sup> MEFs and in control *polk*-expressing MEFs (from “wild-type” *Polk*<sup>+/+</sup> animals) after acquisition of different forms of DNA damage. For comparison, to test the role of *polη* in S-phase checkpoint regulation, we compared rates of DNA synthesis in TERT-immortalized XPV fibroblasts (derived from *polη*-deficient XPV patients) with an isogenic cell line stably expressing reconstituted *polη* cDNA. The results of these experiments are shown in Fig. 5.

As expected, 100 nM BPDE elicited a transient inhibition of DNA synthesis in WT MEFs, which recovered from the S-phase arrest 4–6 h following genotoxin treatment. After BPDE-treatment, rates of DNA synthesis were inhibited with similar kinetics in WT and *Polk*<sup>-/-</sup> MEFs (Fig. 5*a*). Interestingly however, *polk*-deficient cells failed to recover from the intra-S-phase checkpoint (Fig. 5*a*). In contrast, *polη*-deficiency (in XPV cells) did not affect recovery from BPDE-induced S-phase arrest (Fig. 5*a*). These data demonstrate a specific requirement for *polk* in recovery from the BPDE-induced S-phase checkpoint.

We next asked if defective recovery from the intra-S-phase checkpoint in *Polk*<sup>-/-</sup> cells was specific for BPDE-induced lesions. Therefore, we determined the checkpoint responses to UVC, IR, and hydroxyurea in WT and *Polk*<sup>-/-</sup> cells and in XPV and XPV+ *polη* cells. Similar to results of thymidine incorporation experiments after BPDE treatment, *Polk*<sup>-/-</sup> cells showed defective recovery from UVC-induced growth arrest (Fig. 5*b*). Recovery from the UV light-induced S-phase checkpoint was also defective in XPV cells relative to the isogenic expressing reconstituted *polη*. However, recovery from hy-

droxyurea and IR-induced inhibition of DNA synthesis was unimpaired in cells lacking *polk* or *polη* (Fig. 5, *c* and *d*). Taken together, these data suggest that *polk* is important for recovery from the S-phase checkpoint induced by bulky BPDE adducts and pyrimidine dimers (or other forms of UV light-induced damage) but that there is not a general defect in recovery from S-phase arrest in *Polk*<sup>-/-</sup> cells. In contrast, *polη* is necessary for recovery from UV light-induced S-phase arrest, but not from checkpoints induced by BPDE, IR, or hydroxyurea.

It was formally possible that the defective recovery of DNA synthesis in BPDE-treated *Polk*<sup>-/-</sup> cells resulted from cell cycle effects in G<sub>1</sub> or G<sub>2</sub>/M rather than failure of S-phase-arrested cells to resume DNA synthesis after genotoxin treatment. To eliminate this possibility, we specifically compared the progression of S-phase populations in WT and *Polk*<sup>-/-</sup> cultures after BPDE treatment. Exponentially growing cells were grown for 30 min in medium containing BrdUrd to label S-phase cells. The cells were washed extensively (to remove unincorporated BrdUrd) and then placed in fresh BrdUrd-free growth medium. We then selectively followed the movement of the BrdUrd-positive (S-phase-arrested) populations after BPDE treatment in the WT and *Polk*<sup>-/-</sup> cells. As shown in Fig. 5*e*, 8 h after BPDE treatment, almost 40% of the S-phase population in WT cells had progressed into G<sub>2</sub>, M, and G<sub>1</sub> of the next cell cycle. In contrast, only 6% of the S-phase population of *Polk*<sup>-/-</sup> cells progressed into subsequent stages of the cell cycle 8 h after BPDE treatment. Therefore, *polk* is required for resumption of S-phase progression after BPDE-induced S-phase arrest.

The *Polk*<sup>+/+</sup> and *Polk*<sup>-/-</sup> MEF cultures consist of heteroge-

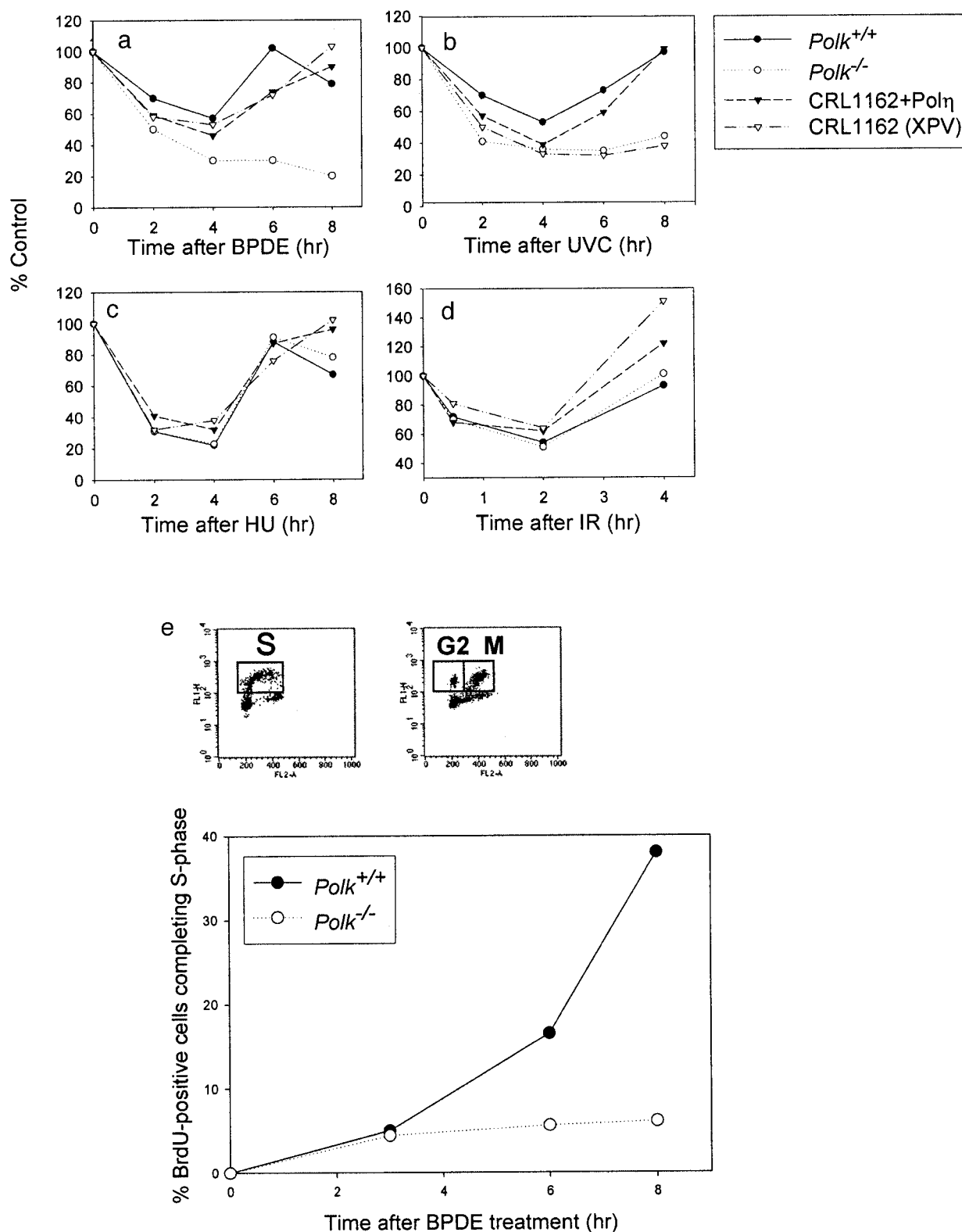
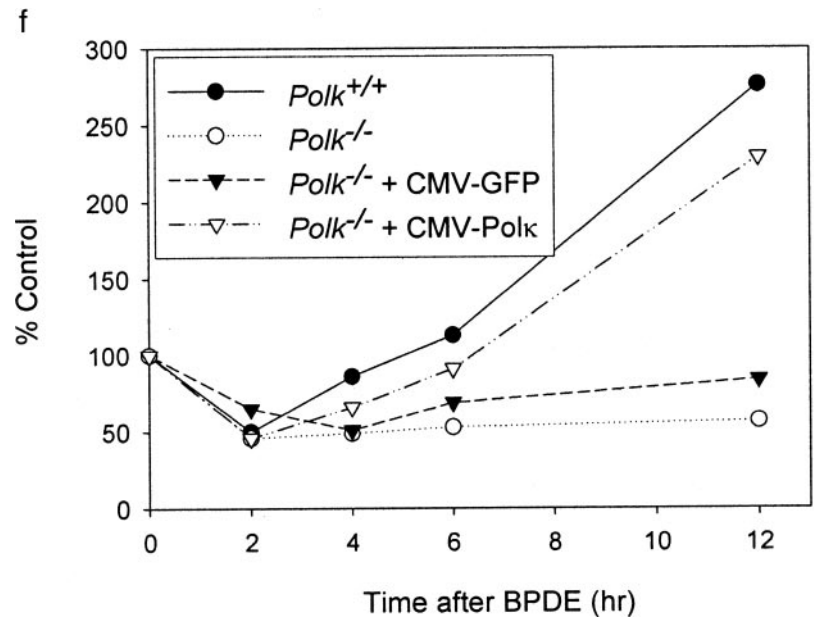


**FIG. 5. Effect of different genotoxin treatments on DNA synthesis in *Polk*<sup>+/+</sup>, *Polk*<sup>-/-</sup>, XPV, and XPV + *pol*η cells.** *Polk*<sup>-/-</sup>, *Polk*<sup>+/+</sup>, CRL1162 (XPV), and CRL1162 + *pol*η cells were treated with 100 nM BPDE (a), 10 J/cm<sup>2</sup> UVC (b), 1 mM hydroxyurea for 1 h (c), or 5 gray IR (d). After genotoxin treatments, the culture medium was replenished, and the rates of DNA synthesis in replicate cultures were determined by measurement of radiolabeled thymidine incorporation at the indicated time points. The percentage of DNA synthesis for treated samples relative to that for the corresponding untreated control is shown. e, for "relative movement" assays, *Polk*<sup>-/-</sup> and *Polk*<sup>+/+</sup> cells were pulsed with BrdUrd for 1 h to label the S-phase population. The resulting cultures were washed to remove unincorporated BrdUrd and then treated with 100 nM BPDE. At various times after BPDE treatment, cells were harvested for FACS analysis. The relative movement of BrdUrd-positive nuclei into G<sub>2</sub>/M and G<sub>1</sub> of the subsequent cell cycle was determined for each sample and expressed as a percentage of the total population (right panel). The panel on the right side of the figure indicates the gates used to identify the G<sub>1</sub> and G<sub>2</sub>/M populations. f, *Polk*<sup>-/-</sup> cells were transfected with 3 μg of CMV-GFP or CMV-*pol*κ plasmids using Lipofectamine 2000. Transfection efficiency was estimated at >80% based on GFP fluorescence of CMV-GFP-transfected cells. Untransfected WT cells and CMV-GFP or CMV-*pol*κ-transfected cultures were treated with 100 nM BPDE. At various times after BPDE treatment, rates of DNA synthesis were determined by measurements of [<sup>3</sup>H]thymidine incorporation.



FIG. 5—continued



neous populations of cells. Therefore, it was possible that the defective recovery of *Polk*<sup>-/-</sup> cultures from genotoxin-induced S-phase checkpoint resulted from *Polk*-independent differences between the WT and *Polk*<sup>-/-</sup> cell lines. To test this possibility, we transiently transfected a *polκ* expression vector (or a GFP expression plasmid for control) into *Polk*<sup>-/-</sup> MEFs and then tested the effect of *polκ* reconstitution on the S-phase checkpoint. As shown in Fig. 5f, *Polk*<sup>-/-</sup> cultures transfected with a control (CMV-GFP) expression vector failed to recover from 100 nM BPDE-induced inhibition of DNA synthesis. In contrast, in parallel cultures of *Polk*<sup>-/-</sup> cells transfected with a CMV-driven *polκ* expression plasmid (CMV-*polκ*) DNA synthesis was inhibited transiently 2 h after treatment with 100 nM BPDE. Similar to WT cells, CMV-*polκ*-reconstituted *Polk*<sup>-/-</sup> MEFs recovered from S-phase arrest 4–6 h following BPDE treatment (Fig. 5f). In similar experiments using WT cells, ectopically expressed *polκ* had no effect on the kinetics of inhibition of DNA synthesis or recovery from S-phase arrest (data not shown). Taken together, these data show that reconstitution of *polκ* expression specifically corrects the checkpoint defect in *Polk*<sup>-/-</sup> cells.

***polκ*-deficient Cells Are Highly Sensitive to BPDE**—Defective S-phase checkpoints are often associated with decreased viability. Indeed, recovery from replication stress is considered to be the essential role of S-phase checkpoints (43). To test if defective recovery of *Polk*<sup>-/-</sup> cells from the S-phase checkpoint correlated with genotoxin sensitivity, we determined the effect of different DNA-damaging agents on the viability of WT and *Polk*<sup>-/-</sup> MEFs. Exponentially growing MEFs were given different genotoxins or were left untreated. 24 h later, control and genotoxin-treated cells were trypsinized, counted, and replated at a density of 1000 cells/10-cm dish. 10 days later, colonies resulting from the surviving cells were fixed, stained with crystal violet, and counted. The effects of different treatments on clonogenic survival of WT and *Polk*<sup>-/-</sup> MEFs are shown in Fig. 6.

We saw little or modest differences between survival of WT and *polκ*-deficient cells after treatments with hydroxyurea or IR. Most interestingly, however, treatment with 100 nM BPDE resulted in no loss of viability of WT cells but elicited a 70% decrease in clonogenic survival of *Polk*<sup>-/-</sup> MEFs. These data demonstrate that *polκ* is important for cell survival after BPDE treatment.

*polκ* deficiency also had a modest inhibitory effect on survival after 10–20 J/m<sup>2</sup> UVC treatment. Although 20 J/m<sup>2</sup> UVC elicited a 50% inhibition of colony formation in WT cells, the same dose resulted in 80% reduction in clonogenic survival of *Polk*<sup>-/-</sup> cells (Fig. 6). These results are consistent with previous work that showed a moderate increase in UV light sensitivity of *Polk*<sup>-/-</sup> embryonic stem and MEF cells relative to WT controls (29, 44). Therefore, our results show a requirement for *polκ* for cell survival after acquisition of BPDE adducts and also UV light adducts.

**Checkpoint Signaling Responses to BPDE in *polκ*-deficient Cells**—The checkpoint kinase Chk1 is activated in response to replication blocks. We have shown previously that Chk1 mediates the BPDE-induced S-phase checkpoint (32). We determined the effects of BPDE on Chk1 signaling in WT and *Polk*<sup>-/-</sup> MEFs. As expected, 100 nM BPDE induced a transient phosphorylation of Chk1 on Ser-345 (indicative of active Chk1) in WT cells (Fig. 7a, 1- and 4-h time points), concomitant with inhibition of DNA synthesis (see Fig. 5a). However, 8 h after 100 nM BPDE treatment, Chk1 phosphorylation had returned to near-basal levels (Fig. 7a). In contrast, in a parallel experiment performed with *Polk*<sup>-/-</sup> cells, BPDE induced higher levels of Chk1 phosphorylation. Moreover, in *Polk*<sup>-/-</sup> cells, BPDE-induced Chk1 phosphorylation was sustained for the entire duration of the experiment (Fig. 7a, 1-, 4-, 8-, 12-, and 24-h time points). The prolonged phosphorylation of Chk1 in response to 100 nM BPDE in *Polk*<sup>-/-</sup> cells is indicative of sustained replication blocks and is consistent with our DNA synthesis assays showing defective recovery from the BPDE-induced S-phase checkpoint (see Fig. 5a). Taken together, these data suggest that in *polκ*-deficient cells replication forks remain stalled and activate Chk1 persistently after encountering BPDE lesions.

BPDE adducts do not generate DNA double strand breaks (DSBs) directly; however, of the single-stranded DNA regions caused by persistent blockage of the leading strand and uncoupling of lagging strand synthesis may result in formation of DSBs (45). We hypothesized that the increased numbers of stalled forks in BPDE-treated *Polk*<sup>-/-</sup> cells relative to wild-type MEFs might generate DSBs. Therefore, we determined the levels of histone  $\gamma$ H2AX, an early marker of DSB formation, in WT and *Polk*<sup>-/-</sup> cells after 100 nM BPDE treatment. As shown in Fig. 7c, we detected sustained levels of histone  $\gamma$ H2AX in *Polk*<sup>-/-</sup> cells after treatment with BPDE, consistent

**FIG. 6. Effect of different genotoxins on clonogenic survival of *Polk*<sup>+/+</sup> and *Polk*<sup>-/-</sup> cells.** Replicate plates of exponentially growing *Polk*<sup>-/-</sup> and *Polk*<sup>+/+</sup> cells were treated with different genotoxins as indicated. 24 h later, control and genotoxin-treated cells were trypsinized and re-plated on 10-cm plates at a density of 1000 cells/plate. The growth medium on the re-plated cells was replenished every 3 days. After 10 days, colonies of cells present on the plates were stained with crystal violet and enumerated. The bar graph indicates the number of colonies on each plate expressed as a percentage of the number of colonies on plates derived from control untreated cultures. Gy, gray.

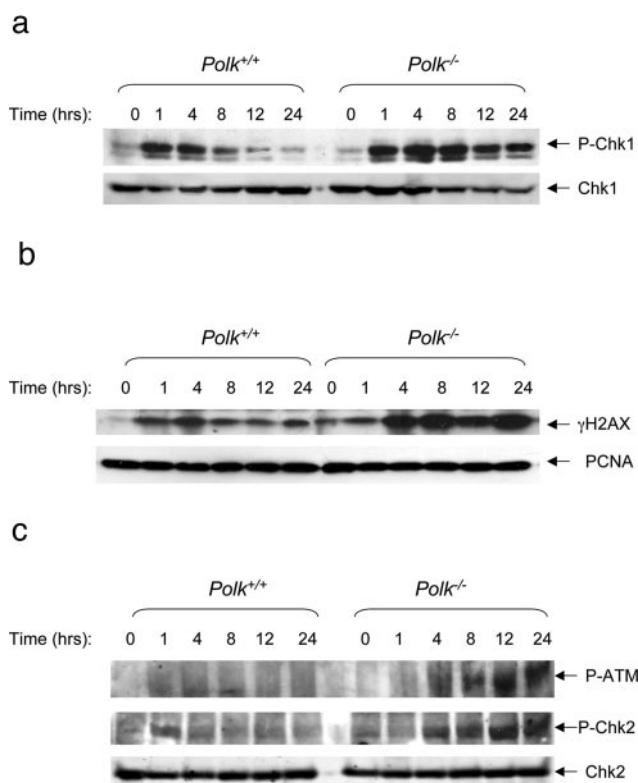
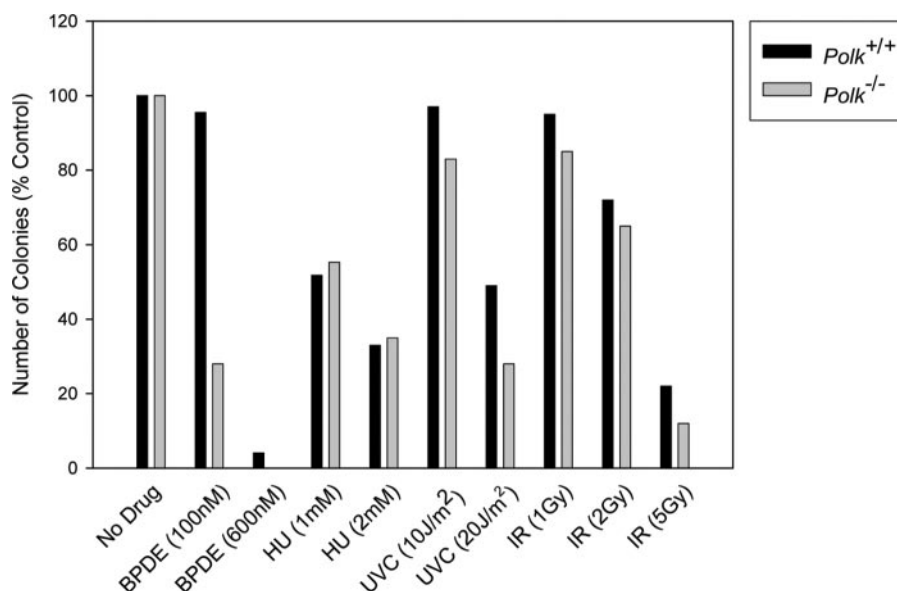


**FIG. 7. Effect of BPDE on phosphorylation of ATM, checkpoint kinases, and  $\gamma$ H2AX in *Polk*<sup>+/+</sup> and *Polk*<sup>-/-</sup> cells.** Exponentially growing *Polk*<sup>+/+</sup> and *Polk*<sup>-/-</sup> cells were treated with 100 nM BPDE. At the indicated time points after BPDE treatment, total cell lysates (or washed nuclei for PCNA and H2AX blots) were prepared, separated by SDS-PAGE, and immunoblotted sequentially with antisera against phosphoserine 345-Chk1 and total Chk1 (a), H2AX and PCNA (b), or phosphoserine 1981 ATM, phosphothreonine 78 Chk2, and total Chk2 (c).

with the formation of DSBs as a result of *polk* deficiency.

Although bulky adducts such as BPDE and UV light activate the S-phase checkpoint via the ATR/Chk1 pathway, DSBs elicit a distinct S-phase checkpoint mechanism mediated by the ATM and Chk2 kinases (18). Active forms of ATM and Chk2 can be detected readily by using phospho-specific antibodies. We used phospho-specific antisera to determine the activation status of ATM and Chk2 in WT and *Polk*<sup>-/-</sup> cells after treatment with 100 nM BPDE. As shown in Fig. 7b, we saw little

change in ATM or Chk2 phosphorylation in WT cells after BPDE treatment. The lack of ATM/Chk2 activation by BPDE in WT cells is consistent with our previous findings that ATM and Chk2 are dispensable for the BPDE-induced S-phase checkpoint (32). In contrast with WT MEFs, we detected large increases in ATM and Chk2 phosphorylation in *Polk*<sup>-/-</sup> cells 8–12 h after BPDE treatment (Fig. 7b). Taken together, these results suggest that *polk* is required for recovery from BPDE-induced S-phase arrest (Fig. 8). In the absence of *polk*, replication forks most likely remain stalled at sites of BPDE lesions. Stalled forks ultimately give rise to DSBs that elicit H2AX phosphorylation and additional ATM/Chk2-mediated events (Fig. 8).

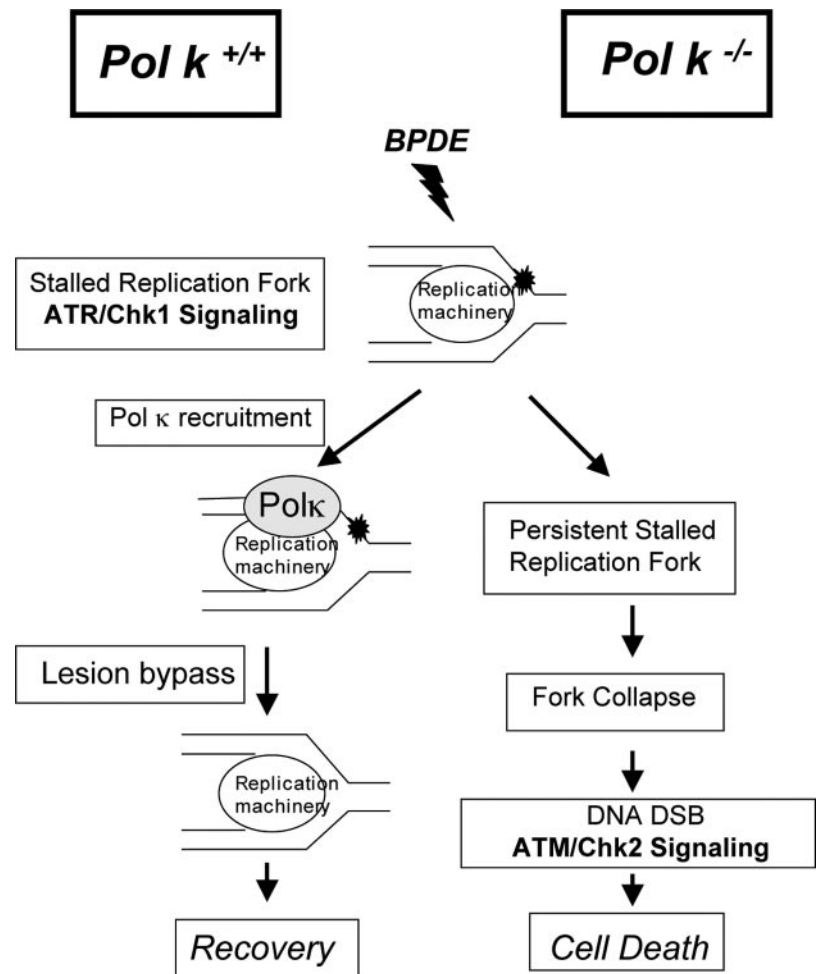
#### DISCUSSION

In this report we have investigated the roles of the TLS enzymes *polk* and *polη* in the S-phase checkpoint elicited by the carcinogen BPDE. Our results show that *polk* is recruited to nuclear foci in response to BPDE treatment. Recovery from BPDE-induced S-phase arrest is normal in XPV cells, indicating that *polη* is dispensable for the BPDE-induced S-phase checkpoint. However, in contrast with WT MEFs, which recover from BPDE-induced inhibition of DNA synthesis, BPDE-treated *Polk*<sup>-/-</sup> MEF cells undergo a sustained replication block. BPDE-induced inhibition of DNA synthesis in *Polk*<sup>-/-</sup> cells is associated with increased levels of  $\gamma$ H2AX (a marker of DSBs) as well as activation of ATM/Chk2 kinases, known mediators of the response to DSBs. Taken together, these results suggest that *polk* is required for bypass of BPDE lesions, thereby enabling recovery from bulky adduct-induced S-phase checkpoint. In the absence of DNA *polk*, replication forks stalled at bulky lesions generate DSBs that induce secondary checkpoint signaling events and loss of viability (Fig. 8).

Most interestingly, Cleaver and co-workers (46) have shown that UV irradiation leads to the formation of  $\gamma$ H2AX and Mre11 foci in XP-V fibroblasts but not in normal cells. Taken together, it appears that during S-phase *polk* and *polη* are required for bypass of BPDE- and UV light-induced lesions, respectively. Failure to bypass BPDE- or UV light-induced adducts in *polk*- or *polη*-deficient cells leads to fork collapse and DSBs.

In a recent study, Livneh and co-workers (47) quantified TLS across a BPDE-dG adduct in cells from WT and *Polk*<sup>-/-</sup> mice. Most interestingly, TLS of the BPDE-dG adduct in *Polk*<sup>-/-</sup> cells occurred with 1/3 the efficiency of that observed in WT

FIG. 8. Hypothetical model describing role of *polk* in the BPDE-induced S-phase checkpoint. In WT cells, replication forks that encounter BPDE lesions induce ATR/Chk1 signaling and transient S-phase arrest. *polk* is recruited to stalled replication forks and the ensuing translesion DNA replication enables recovery from the S-phase checkpoint. In *polk*-deficient cells, stalled forks persist at sites of DNA lesions. Stalled forks ultimately collapse to generate DSBs that induce ATM/Chk2 signaling.



cells, suggesting that at least 2/3 of the BPDE-dG adducts in MEFs were bypassed exclusively by *polk* *in vivo*. In contrast, *polη* was not required for bypass across BPDE-dG adduct (47). These data are consistent with our results that *polk* (but not *polη*) is required for recovery from the intra-S-phase checkpoint induced by BPDE.

Because *polk* can perform TLS of BPDE adducts *in vitro* and *in vivo*, *polk*-dependent recovery from the S-phase checkpoint most likely occurs via TLS of BPDE-adducts encountered by the replication fork. Similarly, *polη* can bypass TT-adducted templates *in vitro*, and the *polη*-mediated TLS of UV light-induced DNA lesions at the replication fork is likely to be important for recovery from the UV light-induced S-phase checkpoint. Therefore, it is unexpected that *polk* (which cannot bypass TT dimers *in vitro*) is required for recovery from UV light-induced S-phase arrest. This result might suggest that there is a requirement for *polk* in TLS of UV light-induced lesions *in vivo*. A putative role for *polk* in the UV light response has been suggested previously. For example, *Polk*-null embryonic stem and MEF cells were shown to be sensitive to UV light (29, 44). Moreover, although *polk* shows no ability to replicate past a *cis-syn* T-T dimer, Prakash and co-workers (48, 49) have shown that *polk* is an extender in TLS, efficiently extending from a G opposite the 3' T of a TT dimer. Therefore, consistent with a TLS-based mechanism for recovery from the UV light-induced S-phase checkpoint, *polk* might be required for TLS of UV light-induced lesions *in vivo*.

However, this model does not explain why *polη* is unable to perform TLS of UV lesions in a *Polk*<sup>-/-</sup> background (yet purified *polη* bypasses TT dimers efficiently *in vitro*). One plausible explanation is that *polk* is an important accessory factor that is

needed for optimal *polη*-mediated TLS *in vivo*. Undoubtedly, the complexity of TLS *in vivo* has not been recapitulated *in vitro*. For example, whereas mono-ubiquitinated PCNA is essentially required for *polη*-mediated TLS *in vivo* (25, 26), an *in vitro* study has reported that bypass of TT dimers by *polη* was significantly enhanced by unmodified PCNA (50).

Therefore, although *polη* alone can bypass TT lesions *in vitro*, it is possible that *polk* is required for some aspect of *polη* function *in vivo*. Consistent with functional interactions between *polk* and *polη*, both polymerases co-localize with the TLS enzyme Rev1 at DNA damage-induced subnuclear foci *in vivo* (40, 51). It has been suggested that a TLS complex comprising multiple polymerases (including *polk* and *polη*) travels behind the replication fork in anticipation of possible fork-blocking lesions (52). It is possible that *polk* deficiency compromises the function of *polη* or other components of the putative TLS complex.

Alternatively, it is possible that the critical role of *polk* in recovery from the S-phase checkpoint is not mediated via TLS activity. Instead, *polk* might transmit a negative regulatory signal to the relevant checkpoint pathways (ATR, 9-1-1, and Chk1) that enables recovery from the S-phase arrest. In *S. cerevisiae*, Dpb2 mediates interactions between the non-catalytic C-terminal domain of DNA *polε* and the checkpoint-/replication protein Dpb11 (53, 54). Also, in yeast and *Xenopus* systems, *polα* primase is an important target for S-phase checkpoint control (55–57). Based on our studies and emerging evidence from other laboratories, it is likely that TLS polymerases are also integral components of the S-phase checkpoint.

An important unanswered question regarding the role of *polk* in the response to BPDE (and other genotoxins) is the



mechanism of its recruitment to sites of DNA damage. Our observation that caffeine abrogates formation of DNA damage-induced polk foci initially suggested a potential role for the ATM/ATR kinases in recruiting polk to DNA lesions encountered by the replication fork. However, we have not observed defective genotoxin-induced recruitment of GFP-polk to nuclear foci in ATM- or ATR-deficient cells (data not shown). Therefore, we do not believe that the effect of caffeine on GFP-polk localization is mediated via inhibition of ATM/ATR. Nevertheless, our results might help explain the well documented sensitivity of UV light-treated XPV cells to caffeine (41). We have shown here that both polk and pol $\eta$  are involved in recovery from the UV light-induced S-phase checkpoint. If polk and pol $\eta$  have partially overlapping or redundant roles in the response to UV light, polk might be expected to assume a more important role in the UV response in the context of an XPV cell. Therefore, perturbation of polk regulation by caffeine might be expected to have a more dramatic effect on cell survival in a pol $\eta$ -deficient genetic background. Another possibility is that a caffeine-sensitive recombination repair pathway is induced in UV light-treated XPV cells.

Kai and Wang (58, 59) have suggested a role for checkpoint proteins in recruiting polk to damaged chromatin. In studies with *Schizosaccharomyces pombe*, these workers (58, 59) showed that DinB (polk) binds to Hus1, a component of the Rad9-Rad1-Hus1 (9-1-1) clamp complex, in response to DNA damage. We have shown previously that Hus1 (presumably together with the other components of the 9-1-1 complex) is required for activation of Chk1 and S-phase arrest in response to BPDE in mammalian cells (33). It is formally possible that a conserved 9-1-1-mediated mechanism recruits polk to BPDE lesions in mammalian cells. However, in preliminary experiments, we have shown that polk foci are readily induced by BPDE in cells lacking Rad17, the clamp loader for 9-1-1.<sup>3</sup> This result might suggest that alternative 9-1-1-independent or redundant mechanisms are responsible for recruiting polk to DNA lesions in mammalian cells.

Studies in *S. cerevisiae* have shown that a Rad6/Rad18-mediated ubiquitination of PCNA is important for recruitment of TLS polymerases and for lesion bypass (52, 60). The Lehmann and Yamaizumi laboratories (25, 26) recently demonstrated that this mechanism is important for recruiting pol $\eta$  to sites of UV light-induced lesions. It is therefore possible that a similar Rad6/Rad18-mediated mechanism recruits polk to sites of damage in the context of the S-phase checkpoint elicited by BPDE (and other genotoxins). Experiments are underway to test roles for Rad6/Rad18 in the S-phase checkpoint response and polk regulation.

In this report we have focused on two of the known TLS enzymes, polk and pol $\eta$ , and we have studied their roles in the BPDE-induced S-phase checkpoint. Our results suggest that polk is important for the BPDE- and UV light-induced S-phase checkpoints. However, it is likely that other TLS polymerases are involved in S-phase checkpoint response. Studies from many laboratories indicate that distinct TLS polymerases associate in multiprotein complexes. For example, Kannouche *et al.* (61) have co-localized polk and pol $\eta$  in mammalian cells. Recent studies from multiple groups have demonstrated that internal regions of polk, pol $\eta$ , and pol $\delta$  associate with a C-terminal domain of Rev1 (40, 51, 62). Although the exact significance of these associations is not known, these results suggest cooperative effects of TLS polymerases *in vivo*. Consistent with hypothetical mechanisms involving cooperativity between different TLS enzymes, some reconstitution studies with purified

proteins have demonstrated that distinct polymerases can mediate insertion and extension steps during replicative bypass. It was surprising to us that both BPDE and UV light-induced checkpoints are defective in polk-deficient cells because polk is able to bypass BPDE adducts, but not TT dimers, *in vitro*. As noted above, this result might indicate a more complex interplay between different TLS enzymes *in vivo* than is suggested by *in vitro* studies.

Most interestingly, Rev1 has a BRCT (BRCA1 C-terminal) motif common to many checkpoint signaling and DNA repair proteins (63). Because Rev1 can associate with multiple Y family members (polk, polt, and pol $\eta$ ), it is tempting to speculate that Rev1 is directly linked to checkpoint signaling pathways and is central to recruitment of appropriate TLS enzymes to specific DNA lesions. Clearly, further studies are necessary to define the roles of different TLS enzymes in checkpoint responses to BPDE and other genotoxins. Additional experiments are underway to elucidate the molecular basis for interactions between checkpoint signaling pathways and TLS polymerases in the response to BPDE adducts acquired during S-phase.

**Acknowledgments**—We are grateful to Dr. Bill Kaufmann (University of North Carolina, Chapel Hill) for providing the TERT-immortalized XPV cells. We thank Dr. Tomoo Ogi for sending us WT and *Polk*<sup>-/-</sup> MEFs. We thank Dr. Tomoo Ogi and Dr. Robert Weiss for critical reading of the manuscript. We thank Dr. Beth Sullivan for help with Deltavision microscopy.

## REFERENCES

- Baum, E. J. (1978) in *Polycyclic Hydrocarbons and Cancer: Environment, Chemistry and Metabolism* (Gelboin, H. V., ed) pp. 45–70, Academic Press, New York
- Hemminki, K., Koskinen, M., Rajaniemi, H., and Zhao, C. (2000) *Regul. Toxicol. Pharmacol.* **32**, 264–275
- Hemminki, K. (1993) *Carcinogenesis* **14**, 2007–2012
- Zhou, B. B., and Elledge, S. J. (2000) *Nature* **408**, 433–439
- Falck, J., Petrini, J. H., Williams, B. R., Lukas, J., and Bartek, J. (2002) *Nat. Genet.* **30**, 290–294
- Chen, Y., and Sanchez, Y. (2004) *DNA Repair (Amst.)* **3**, 1025–1032
- Bakkenist, C. J., and Kastan, M. B. (2003) *Nature* **421**, 499–506
- Cortez, D., Guntuku, S., Qin, J., and Elledge, S. J. (2001) *Science* **294**, 1713–1716
- Zou, L., and Elledge, S. J. (2003) *Science* **300**, 1542–1548
- Rauen, M., Burtelow, M. A., Dufault, V. M., and Karnitz, L. M. (2000) *J. Biol. Chem.* **275**, 29767–29771
- Roos-Mattijs, P., Vroman, B. T., Burtelow, M. A., Rauen, M., Eapen, A. K., and Karnitz, L. M. (2002) *J. Biol. Chem.* **277**, 43809–43812
- Parrilla-Casteller, E. R., Arlander, S. J., and Karnitz, L. (2004) *DNA Repair (Amst.)* **3**, 1009–1014
- Zou, L., Cortez, D., and Elledge, S. J. (2002) *Genes Dev.* **16**, 198–208
- Liu, Q., Guntuku, S., Cui, X. S., Matsuo, S., Cortez, D., Tamai, K., Luo, G., Carattini-Rivera, S., DeMayo, F., Bradley, A., Donehower, L. A., and Elledge, S. J. (2000) *Genes Dev.* **14**, 1448–1459
- Maidland, N., Falck, J., Lukas, C., Syljuasen, R. G., Welcker, M., Bartek, J., and Lukas, J. (2000) *Science* **288**, 1425–1429
- Sorensen, C. S., Syljuasen, R. G., Falck, J., Schroeder, T., Ronnstrand, L., Khanna, K. K., Zhou, B. B., Bartek, J., and Lukas, J. (2003) *Cancer Cells* **3**, 247–258
- Costanzo, V., Shechter, D., Lupardus, P. J., Cimprich, K. A., Gottesman, M., and Gautier, J. (2003) *Mol. Cell* **11**, 203–213
- Bartek, J., Lukas, C., and Lukas, J. (2004) *Nat. Rev. Mol. Cell Biol.* **5**, 792–804
- Cox, M. M. (2002) *Mutat. Res.* **510**, 107–120
- McGlynn, P., and Lloyd, R. G. (2002) *Nat. Rev. Mol. Cell Biol.* **3**, 859–870
- Kunz, B. A., Straffon, A. F., and Vonnar, E. J. (2000) *Mutat. Res.* **451**, 169–185
- Baynton, K., and Fuchs, R. P. (2000) *Trends Biochem. Sci.* **25**, 74–79
- Ohmori, H., Friedberg, E. C., Fuchs, R. P., Goodman, M. F., Hanaoka, F., Hinkle, D., Kunkel, T. A., Lawrence, C. W., Livneh, Z., Nohmi, T., Prakash, L., Prakash, S., Todo, T., Walker, G. C., Wang, Z., and Woodgate, R. (2001) *Mol. Cell* **8**, 7–8
- Masutani, C., Kusumoto, R., Yamada, A., Dohmae, N., Yokoi, M., Yuasa, M., Araki, M., Iwai, S., Takio, K., and Hanaoka, F. (1999) *Nature* **399**, 700–704
- Kannouche, P. L., Wing, J., and Lehmann, A. R. (2004) *Mol. Cell* **14**, 491–500
- Watanabe, K., Tateishi, S., Kawasui, M., Tsurimoto, T., Inoue, H., and Yamaizumi, M. (2004) *EMBO J.* **23**, 3886–3896
- Ogi, T., Kato, T. J., Kato, T., and Ohmori, H. (1999) *Genes Cells* **4**, 607–618
- Ohmori, H., Ohashi, E., and Ogi, T. (2004) *Adv. Protein Chem.* **69**, 265–278
- Ogi, T., Shinkai, Y., Tanaka, K., and Ohmori, H. (2002) *Proc. Natl. Acad. Sci. U. S. A.* **99**, 15548–15553
- Bergoglio, V., Bavoux, C., Verbiest, V., Hoffmann, J. S., and Cazaux, C. (2002) *J. Cell Sci.* **115**, 4413–4418
- Haracska, L., Unk, I., Johnson, R. E., Phillips, B. B., Hurwitz, J., Prakash, L., and Prakash, S. (2002) *Mol. Cell Biol.* **22**, 784–791
- Guo, N., Faller, D. V., and Vaziri, C. (2002) *Cell Growth & Differ.* **13**, 77–86

<sup>3</sup> X. Bi and C. Vaziri, unpublished data.

33. Weiss, R. S., Leder, P., and Vaziri, C. (2003) *Mol. Cell. Biol.* **23**, 791–803
34. Vaziri, C., Saxena, S., Jeon, Y., Lee, C., Murata, K., Machida, Y., Wagle, N., Hwang, D. S., and Dutta, A. (2003) *Mol. Cell* **11**, 997–1008
35. Izumi, M., Yanagi, K., Mizuno, T., Yokoi, M., Kawasaki, Y., Moon, K. Y., Hurwitz, J., Yatagai, F., and Hanaoka, F. (2000) *Nucleic Acids Res.* **28**, 4769–4777
36. Ogi, T., Kannouche, P., and Lehmann, A. R. (2005) *J. Cell Sci.* **118**, 129–136
37. Kaufmann, W. K., Smith, B. J., and Cordeiro-Stone, M. (1985) *Biochim. Biophys. Acta* **824**, 146–151
38. Cordeiro-Stone, M., Smith, B. J., and Kaufmann, W. K. (1986) *Carcinogenesis* **7**, 1775–1781
39. Kannouche, P., Broughton, B. C., Volker, M., Hanaoka, F., Mullenders, L. H., and Lehmann, A. R. (2001) *Genes Dev.* **15**, 158–172
40. Tissier, A., Kannouche, P., Reck, M. P., Lehmann, A. R., Fuchs, R. P., and Cordonnier, A. (2004) *DNA Repair (Amst.)* **3**, 1503–1514
41. Kaufmann, W. K., Heffernan, T. P., Beaulieu, L. M., Doherty, S., Frank, A. R., Zhou, Y., Bryant, M. F., Zhou, T., Luche, D. D., Nikolaishvili-Feinberg, N., Simpson, D. A., and Cordeiro-Stone, M. (2003) *Mutat. Res.* **532**, 85–102
42. Sarkaria, J. N., Busby, E. C., Tibbetts, R. S., Roos, P., Taya, Y., Karnitz, L. M., and Abraham, R. T. (1999) *Cancer Res.* **59**, 4375–4382
43. Desany, B. A., Alcasabas, A. A., Bachant, J. B., and Elledge, S. J. (1998) *Genes Dev.* **12**, 2956–2970
44. Velasco-Miguel, S., Richardson, J. A., Gerlach, V. L., Lai, W. C., Gao, T., Russell, L. D., Hladik, C. L., White, C. L., and Friedberg, E. C. (2003) *DNA Repair (Amst.)* **2**, 91–106
45. Cleaver, J. E., Laposa, R. R., and Limoli, C. L. (2003) *Cell Cycle* **2**, 310–315
46. Limoli, C. L., Giedzinski, E., Bonner, W. M., and Cleaver, J. E. (2002) *Proc. Natl. Acad. Sci. U. S. A.* **99**, 233–238
47. Avkin, S., Goldsmith, M., Velasco-Miguel, S., Geacintov, N., Friedberg, E. C., and Livneh, Z. (2004) *J. Biol. Chem.* **279**, 53298–53305
48. Haracska, L., Prakash, L., and Prakash, S. (2002) *Proc. Natl. Acad. Sci. U. S. A.* **99**, 16000–16005
49. Washington, M. T., Johnson, R. E., Prakash, L., and Prakash, S. (2002) *Proc. Natl. Acad. Sci. U. S. A.* **99**, 1910–1914
50. Haracska, L., Johnson, R. E., Unk, I., Phillips, B., Hurwitz, J., Prakash, L., and Prakash, S. (2001) *Mol. Cell. Biol.* **21**, 7199–7206
51. Ohashi, E., Murakumo, Y., Kanjo, N., Akagi, J., Masutani, C., Hanaoka, F., and Ohmori, H. (2004) *Genes Cells* **9**, 523–531
52. Ulrich, H. D. (2004) *Cell Cycle* **3**, 15–18
53. Navas, T. A., Sanchez, Y., and Elledge, S. J. (1996) *Genes Dev.* **10**, 2632–2643
54. Navas, T. A., Zhou, Z., and Elledge, S. J. (1995) *Cell* **80**, 29–39
55. Hekmat-Nejad, M., You, Z., Yee, M. C., Newport, J. W., and Cimprich, K. A. (2000) *Curr. Biol.* **10**, 1565–1573
56. You, Z., Kong, L., and Newport, J. (2002) *J. Biol. Chem.* **277**, 27088–27093
57. Michael, W. M., Ott, R., Fanning, E., and Newport, J. (2000) *Science* **289**, 2133–2137
58. Kai, M., and Wang, T. S. (2003) *Mutat. Res.* **532**, 59–73
59. Kai, M., and Wang, T. S. (2003) *Genes Dev.* **17**, 64–76
60. Stelter, P., and Ulrich, H. D. (2003) *Nature* **425**, 188–191
61. Kannouche, P., Fernandez de Henestrosa, A. R., Coull, B., Vidal, A. E., Gray, C., Zicha, D., Woodgate, R., and Lehmann, A. R. (2002) *EMBO. J.* **21**, 6246–6256
62. Guo, C., Fischhaber, P. L., Luk-Paszyc, M. J., Masuda, Y., Zhou, J., Kamiya, K., Kisker, C., and Friedberg, E. C. (2003) *EMBO. J.* **22**, 6621–6630
63. Lawrence, C. W. (2002) *DNA Repair (Amst.)* **1**, 425–435